

# Inflation and eversion of functionally graded non-linear elastic incompressible circular cylinders

R.C. Batra\*, A. Bahrami

Department of Engineering Science and Mechanics, M/C 0219, Virginia Polytechnic Institute and State University, Blacksburg, VA 24061, USA

## ARTICLE INFO

### Article history:

Received 11 September 2008

Received in revised form 8 December 2008

Accepted 19 December 2008

### Keywords:

Non-linear elasticity

Thick cylinder

Radial expansion/contraction

Surface tension

Eversion

## ABSTRACT

We study axisymmetric radial deformations of a circular cylinder composed of an inhomogeneous Mooney–Rivlin material with the two material parameters varying continuously through the cylinder thickness either by a power law or an affine relation. It is found that for the exponent of the power law function equal to 1, the hoop stress for an internally pressurized cylinder is uniform in the cylinder. One can tailor the gradation of these two material parameters to make the maximum tensile hoop stress occur either on the inner surface or on the outer surface. Also, the stress concentration in a pressurized thick cylinder strongly depends upon the value of the exponent of the power law variation of the two material parameters. For an affine through-the-thickness variation of the two elastic moduli the hoop stress at the point  $R = \sqrt{R_{in}R_{ou}}$  is nearly the same as that in a cylinder composed of a homogeneous material. Here  $R_{in}$  and  $R_{ou}$  equal, respectively, the inner and the outer radii of the cylinder in the unstressed reference configuration, and  $R$  is the radial coordinate of a point in the reference configuration. The stress distribution in an everted cylinder strongly depends upon its thickness in the reference configuration.

© 2008 Elsevier Ltd. All rights reserved.

## 1. Introduction

Rubberlike materials are often used to make tires, catheters, water hoses, and shock absorbers. Depending upon the intended application it may be desirable to suitably vary material properties in one or more directions to optimize the life of the part. This can be achieved by either changing the chemical composition or fabricating the component from two or more materials; e.g. see [1].

Rubberlike materials are usually modeled as incompressible non-linear elastic. Simple constitutive relations for studying their mechanical deformations include the neo-Hookean and the Mooney–Rivlin. Batra [2] studied, numerically with the finite element method, plane strain axisymmetric deformations of a circular cylinder made of an inhomogeneous Mooney–Rivlin material with the two material parameters expressed as polynomials of degree one or two in the radial coordinate,  $R$ , in the undeformed configuration. Here we study a similar problem analytically, find surface tension in a thin cylinder loaded by an internal pressure, the stress concentration in a very thick cylinder loaded by an internal pressure, and stress distributions in cylinders with the two material parameters expressed either as power law functions of  $R$  or as affine functions of  $R$ , and

the eversion of a cylinder made of an inhomogeneous material. We adopt a member of Ericksen's family of universal solutions [3] corresponding to radial expansion/contraction of a cylinder made of a hyperelastic material.

Explicit solutions for radial deformations of a cylinder composed of a homogeneous Mooney–Rivlin material have been given by Rivlin [4], who has also analyzed the eversion of a cylindrical tube made of a neo-Hookean material [4]. The present work attempts to illuminate effects of material inhomogeneities on through-the-thickness stress distributions and how to exploit these for optimally designing circular cylinders made of rubberlike materials. For example, it was recently found [5] that for a circular cylinder made of an incompressible isotropic Hookean material, the hoop stress is constant through the cylinder thickness if the shear modulus is a linear function of  $R$ . It is surprising that the same result essentially holds for finite deformations of a cylinder composed of a Mooney–Rivlin material with the two material moduli linear functions of  $R$ . However, it does not hold for a circular cylinder made of a second-order linear elastic incompressible material [6]. Bilgili [7] has analyzed plane strain deformations of a circular cylinder made of an inhomogeneous neo-Hookean material with circumferential displacements prescribed on the inner and the outer surfaces.

Materials whose elastic moduli vary continuously in one or more directions are called functionally graded (FG). A goal is to exploit desirable properties of the constituents so as to optimize the performance of the structure. It is commonly believed that the

\* Corresponding author.

E-mail addresses: [rbatra@vt.edu](mailto:rbatra@vt.edu) (R.C. Batra), [bahrami@vt.edu](mailto:bahrami@vt.edu) (A. Bahrami).

gradation of material properties will enhance the life of the structure since it eliminates the delamination mode of failure often prevalent in laminated composites. However, debonding at interfaces between different constituents can induce cracks and cause structural failure. From mechanics point of view, a structure made of an FG material is inhomogeneous. Thus equations of equilibrium when written in terms of displacements have a body force like term representing the interaction between neighboring particles.

Homogenization techniques for deriving effective material properties of composites with a non-linear elastic material as the matrix have not been fully developed. Lopez-Pamies and Castaneda [8] have used a second-order homogenization method to determine the overall constitutive response of an elastomer reinforced with either rigid or compliant fibers and subjected to finite deformations. Another possibility is to use the rule of mixtures, e.g. see [9], or adopt numerical simulations to deduce the effective material properties of the composite from those of its constituents, e.g. see [10]. Here we assume a continuous variation in the radial direction of the two material parameters in the Mooney–Rivlin constitutive relation, and do not find volume fractions of constituents required to attain these material properties. This is similar to the approach followed by Horgan and Chan [11] who analyzed deformations of FG cylinders composed of compressible isotropic linear elastic materials with only Young's modulus varying in the radial direction according to a power law relation. Whereas an incompressible material can undergo only isochoric deformations a compressible material can admit both isochoric and non-isochoric deformations. Lechnitskii's book [12] has solutions for several problems involving inhomogeneous linear elastic materials. One could divide the thickness of a FG cylinder into several layers, regard material properties in each layer as uniform, and analyze a multi-body problem with tractions and displacement continuity conditions imposed at interfaces between adjoining cylinders. With an increase in the number of layers, the solution for the layered cylinder should approach that for the FG cylinder. For background information on non-linear elasticity, the reader is referred to [13–15,17,18] wherein the problem of radial expansion of a homogeneous cylinder has also been studied.

## 2. Problem formulation

We assume that the cylinder is deformed statically (or very slowly) with pressures  $p_{in}$  and  $p_{ou}$  applied to its inner and outer surfaces, respectively, and it is made of an isotropic and incompressible Mooney–Rivlin material for which

$$\mathbf{T} = -p\mathbf{1} + C_1(R)\mathbf{B} + C_2(R)\mathbf{B}^{-1}. \quad (2.1)$$

Here  $\mathbf{T}$  is the Cauchy stress tensor,  $p$  the hydrostatic pressure not determined by the deformation gradient  $\mathbf{F}$ ,  $\mathbf{B} = \mathbf{F}\mathbf{F}^T$  is the left Cauchy–Green tensor,  $\mathbf{B}^{-1}$  equals the inverse of  $\mathbf{B}$ ,  $\mathbf{1}$  the identity tensor,  $R$  the radial coordinate of a point in the unstressed reference configuration, and  $C_1(R)$  and  $C_2(R)$  are material parameters. For a neo-Hookean material,  $C_2(R) = 0$  in Eq. (2.1).

For infinitesimal deformations

$$\mu(R) = C_1(R) - C_2(R), \quad (2.2)$$

equals the shear modulus.

We use cylindrical coordinates with  $(r, \theta, z)$  denoting coordinates of a material point that in the reference configuration occupied the place  $(R, \Theta, Z)$  with the origin on the cylinder axis and  $0 \leq Z \leq L$ , where  $L$  equals the cylinder length in the reference configuration. Because of the axial symmetry of the cylinder geometry, the material properties and the external loads (or the boundary conditions) we presume that deformations of the cylinder are axisymmetric. Thus displacements of a point and the induced stresses are independent

of the angular position  $\theta$ . The three equations expressing the balance of linear momentum imply that the hydrostatic pressure  $p$  in Eq. (2.1) is a function of  $r$  only.

In the absence of body forces, the balance of linear momentum in the radial direction requires that the physical components of  $\mathbf{T}$  satisfy

$$\frac{\partial T_{rr}}{\partial r} + \frac{\partial T_{rz}}{\partial z} + \frac{T_{rr} - T_{\theta\theta}}{r} = 0. \quad (2.3)$$

The pertinent boundary conditions are

$$T_{rr}|_{r=r_{in}} = -p_{in}, \quad T_{rr}|_{r=r_{ou}} = -p_{ou}, \quad (2.4)$$

where  $r_{in}$  and  $r_{ou}$  are, respectively, the inner and the outer radii of the deformed cylinder. When studying the radial expansion/contraction of a hollow cylinder we assume that surface tractions on the end faces  $Z=0, L$  needed to deform the body are available. For the eversion problem, the inner surface, the outer surface, and the end faces are taken to be traction free.

Because the cylinder is made of an incompressible material, therefore, deformations must also satisfy

$$\det[\mathbf{F}] = 1, \quad (2.5)$$

where  $\mathbf{F}$  is the deformation gradient.

## 3. Solution

We presume that deformations of the cylinder can be written as

$$r = r(R), \quad \theta = \Theta, \quad z = Z/D, \quad D \neq 0, \quad (3.1)$$

where  $D$  is a constant to be determined. The deformation (3.1) is a member of the family of universal solutions proposed by Ericksen [2], and can be produced in every homogeneous, incompressible and isotropic hyperelastic body under the action of surface tractions only. Here we assume that it can be produced in a cylinder made of an inhomogeneous Mooney–Rivlin material.

In linear elasticity one assumes that  $D=1$ , i.e., a plane strain state of deformation prevails. The principle of superposition can be invoked to treat the case of  $D \neq 1$  in linear elasticity. In non-linear elasticity the assumption of  $D=1$  requires that surface tractions varying in the radial direction and as given by the solution of the problem be prescribed at the plane end faces of the cylinder. Henceforth we will refer to this case as plane strain axisymmetric deformations, and tacitly assume that the required surface tractions on the end faces  $z=0, L/D$  can be provided. We note that a precise statement of the St. Venant principle for a non-linear elastic body is not available. Therefore, one cannot assert that different axial tractions with the same resultant force and moment will not affect deformations at points away from the plane end faces.

For the deformation (3.1), physical components of the deformation gradient  $\mathbf{F}$  and the left Cauchy–Green tensor  $\mathbf{B}$  are given by

$$[\mathbf{F}] = \begin{bmatrix} r' & 0 & 0 \\ 0 & \frac{r}{R} & 0 \\ 0 & 0 & \frac{1}{D} \end{bmatrix}, \quad [\mathbf{B}] = \begin{bmatrix} (r')^2 & 0 & 0 \\ 0 & \frac{r^2}{R^2} & 0 \\ 0 & 0 & \frac{1}{D^2} \end{bmatrix}, \quad (3.2)$$

where  $r' = dr/dR$ . For the deformation (3.1) to be isochoric,

$$1 = \det[\mathbf{F}] = \frac{r'r}{DR}.$$

Thus

$$r = (A + DR^2)^{1/2}, \quad R = ((r^2 - A)/D)^{1/2}, \quad (3.3)$$

where  $A$  is a constant to be determined.

### 3.1. Power law variation of $C_1(R)$ and $C_2(R)$

We assume the following power law variation of  $C_1(R)$  and  $C_2(R)$ :

$$C_1(R) = C_{10}(R/R_{in})^m, \quad C_2(R) = C_{20}(R/R_{in})^n, \quad (3.4)$$

where  $C_{10}$  and  $C_{20}$  are constants having units of stress,  $R_{in}$  equals the inner radius of the cylinder in the reference configuration, and  $m$  and  $n$  are non-dimensional real numbers. For a homogeneous material  $m = n = 0$ .

Substitution for  $r'$  from Eq. (3.3) into Eq. (3.2), and for  $\mathbf{B}$  from Eq. (3.2) into Eq. (2.1) gives

$$[T] = -p \begin{bmatrix} 1 & 0 & 0 \\ 0 & 1 & 0 \\ 0 & 0 & 1 \end{bmatrix} + C_{10} \left( \frac{R}{R_{in}} \right)^m \begin{bmatrix} \frac{D^2 R^2}{r^2} & 0 & 0 \\ 0 & \frac{r^2}{R^2} & 0 \\ 0 & 0 & \frac{1}{D^2} \end{bmatrix} + C_{20} \left( \frac{R}{R_{in}} \right)^n \begin{bmatrix} \frac{r^2}{D^2 R^2} & 0 & 0 \\ 0 & \frac{R^2}{r^2} & 0 \\ 0 & 0 & D^2 \end{bmatrix}. \quad (3.5)$$

Substitution for  $R$  from Eq. (3.3)<sub>2</sub> into Eq. (3.5) and the result into Eq. (2.3) gives

$$\frac{dT_{rr}}{dr} + \frac{1}{r} \left[ C_{10} \left( \frac{R}{R_{in}} \right)^m \left( \frac{D^2 R^2}{r^2} - \frac{r^2}{R^2} \right) + C_{20} \left( \frac{R}{R_{in}} \right)^n \left( \frac{r^2}{D^2 R^2} - \frac{R^2}{r^2} \right) \right] = 0, \quad (3.6)$$

whose integral is

$$T_{rr} = -p_{in} - \frac{C_{10}}{R_{in}^m} \int_{r_{in}}^r \frac{R^m}{r} \left( \frac{D^2 R^2}{r^2} - \frac{r^2}{R^2} \right) dr - \frac{C_{20}}{R_{in}^n} \int_{r_{in}}^r \frac{R^n}{r} \left( \frac{r^2}{D^2 R^2} - \frac{R^2}{r^2} \right) dr. \quad (3.7)$$

From Eq. (3.5) we get

$$T_{\theta\theta} = T_{rr} + C_{10} \left( \frac{R}{R_{in}} \right)^m \left( \frac{r^2}{R^2} - \frac{D^2 R^2}{r^2} \right) + C_{20} \left( \frac{R}{R_{in}} \right)^n \left( \frac{R^2}{r^2} - \frac{r^2}{D^2 R^2} \right), \quad (3.8_1)$$

$$T_{zz} = T_{rr} + C_{10} \left( \frac{R}{R_{in}} \right)^m \left( \frac{1}{D^2} - \frac{D^2 R^2}{r^2} \right) + C_{20} \left( \frac{R}{R_{in}} \right)^n \left( D^2 - \frac{r^2}{D^2 R^2} \right). \quad (3.8_2)$$

Thus knowing  $T_{rr}$  and values of constants  $A$  and  $D$  in Eq. (3.3) one can find  $T_{\theta\theta}$  and  $T_{zz}$ .

Constants  $A$  and  $D$  are to be determined from boundary conditions (2.4)<sub>2</sub> and the resultant equal and opposite axial force  $F_a$  applied at the end faces  $z = 0, L/D$ . That is,  $A$  and  $D$  are solutions of

$$p_{ou} - p_{in} = \frac{C_{10}}{R_{in}^m} \int_{r_{in}}^{r_{ou}} \frac{R^m}{r} \left( \frac{D^2 R^2}{r^2} - \frac{r^2}{R^2} \right) dr + \frac{C_{20}}{R_{in}^n} \int_{r_{in}}^{r_{ou}} \frac{R^n}{r} \left( \frac{r^2}{D^2 R^2} - \frac{R^2}{r^2} \right) dr \equiv g_1(m, n, R_{in}, R_{ou}, A, D),$$

$$F_a = 2\pi \int_{r_{in}}^{r_{ou}} T_{zz} r dr \equiv g_2(m, n, R_{in}, R_{ou}, A, D). \quad (3.9)$$

By the implicit function theorem, these two non-linear algebraic equations have a solution if and only if

$$\det \begin{bmatrix} \frac{\partial g_1}{\partial A} & \frac{\partial g_1}{\partial D} \\ \frac{\partial g_2}{\partial A} & \frac{\partial g_2}{\partial D} \end{bmatrix} \neq 0.$$

The solution of the problem involving the eversion of a cylindrical tube with free ends involves finding  $A$  and  $D$  by solving Eqs. (3.9)<sub>1</sub> and (3.9)<sub>2</sub> with  $p_{in} = p_{ou} = 0$  and  $F_a = 0$ .

The hoop stress,  $T_{\theta\theta}$ , has an extreme value either at  $r = r_{in}$  or at  $r = r_{ou}$  or at an interior point where

$$0 = \frac{dT_{\theta\theta}}{dr} = \frac{1}{r} \frac{d}{dr} \left( r^2 \frac{dT_{rr}}{dr} \right) = \left( -\frac{1}{r} \right) \frac{d}{dr} \left[ C_{10} \left( \frac{R}{R_{in}} \right)^m \left( \frac{D^2 R^2}{r} - \frac{r^3}{R^2} \right) + C_{20} \left( \frac{R}{R_{in}} \right)^n \left( \frac{r^3}{D^2 R^2} - \frac{R^2}{r} \right) \right]. \quad (3.10)$$

Here we have used Eqs. (2.3) and (3.7). For given values of  $A, D, m$  and  $n$ , one can solve Eq. (3.10) for the radial coordinate  $r$  where the hoop stress has an extreme value. Alternatively, one can fix  $r$  and find values of  $m$  or  $n$  from Eq. (3.10).

*Solid cylinder subjected to external pressure:* For a solid circular cylinder with pressure applied on the outer surface, points on the centroidal axis  $R = 0$  cannot move radially. Therefore,  $A = 0$  in Eq. (3.3) and the deformation is described by  $r = \sqrt{D}R$ . Eqs. (2.1), (3.2) and (2.4)<sub>2</sub> give

$$T_{rr} = T_{\theta\theta} = -\hat{p} + C_{10} D^{(1-m/2)} \left( \frac{r}{R_{ou}} \right)^m + C_{20} D^{-(1+n/2)} \left( \frac{r}{R_{ou}} \right)^n,$$

$$T_{zz} = -\hat{p} + C_{10} D^{-(2+m/2)} \left( \frac{r}{R_{ou}} \right)^m + C_{20} D^{(2-n/2)} \left( \frac{r}{R_{ou}} \right)^n,$$

$$\hat{p} = p_{ou} + C_{10} D + \frac{C_{20}}{D}.$$

The constant  $D$  is determined from the resultant of axial tractions applied at the end faces of the cylinder. The cylinder's deformations are homogeneous; however, the stress distribution in it is non-uniform because the cylinder material is inhomogeneous.

#### 3.1.1. Plane strain axisymmetric deformations (i.e., $D = 1$ ) of an FG cylinder with $m = n$

For  $m = n$ , Eqs. (3.8)<sub>1</sub> and (3.8)<sub>2</sub> simplify to the following two equations:

$$T_{\theta\theta} = T_{rr} + \mu_0 \left( \frac{R}{R_{in}} \right)^m \left( \frac{r^2}{R^2} - \frac{R^2}{r^2} \right), \quad (3.11)$$

$$T_{zz} = T_{rr} + \left( \frac{R}{R_{in}} \right)^m \left[ C_{10} \left( 1 - \frac{R^2}{r^2} \right) + C_{20} \left( 1 - \frac{r^2}{R^2} \right) \right],$$

$$\mu_0 = C_{10}(1 - C_{20}/C_{10}). \quad (3.12)$$

For  $\mu_0 > 0$ ,  $T_{\theta\theta} > T_{rr}$  whenever  $A > 0$ . That is, at any point in the FG cylinder with  $m = n$  and undergoing radial expansion the hoop stress is greater than the radial stress.

Let  $[[p]] = p_{in} - p_{ou}$  denote the pressure difference between the inner and the outer surfaces of the cylinder. Then, from Eqs. (2.4)<sub>2</sub>

and (3.7) we get

$$\begin{aligned} \llbracket p \rrbracket &= -\frac{\mu_0}{R_{in}^m} \int_{r_{in}}^{r_{ou}} \frac{R^m}{r} \left( \frac{R^2}{r^2} - \frac{r^2}{R^2} \right) dr \\ &= \frac{\mu_0}{R_{in}^m} A \int_{R_{in}}^{R_{ou}} \frac{(A + 2R^2)}{(A + R^2)^2} R^{m-1} dR. \end{aligned} \tag{3.13}$$

We define the thickness parameter  $a$  and the expansion ratio  $\lambda$  by

$$a = \frac{R_{ou}}{R_{in}}, \quad \lambda = \frac{r_{ou}}{R_{ou}}. \tag{3.14}$$

Thus

$$r_{ou} = \lambda a R_{in}, \quad r_{in} = ((\lambda^2 - 1)a^2 + 1)^{1/2} R_{in}, \quad A = (\lambda^2 - 1)a^2 R_{in}^2. \tag{3.15}$$

For a given thickness parameter  $a$ , and the exponent  $m$  in Eq. (3.13), the pressure difference  $\llbracket p \rrbracket$  is a function of the expansion ratio  $\lambda$ .

For a thin cylinder,

$$\begin{aligned} \llbracket p \rrbracket &= T_{rr}|_{r=r_{ou}} - T_{rr}|_{r=r_{in}} \\ &\simeq \frac{dT_{rr}}{dr} \Big|_{r=r_{in}} (r_{ou} - r_{in}) \\ &= \frac{\mu_0}{r_{in}} \left( \frac{r_{in}^2}{R_{in}^2} - \frac{R_{in}^2}{r_{in}^2} \right) h, \end{aligned} \tag{3.16}$$

where  $h=r_{ou}-r_{in}$  is the thickness of the cylinder in the deformed configuration, and we have neglected second- and higher-order terms in the Taylor series expansion of  $T_{rr}(r)$  about  $r=r_{in}$ . Here we have set material properties of a thin cylinder equal to those of the material on its inner surface which disregards their through-the-thickness variation. Another possibility is to average them over the thickness, e.g. see [20], and account for the change of material properties through the thickness of the cylinder.

Let the surface tension, per unit axial length in the deformed configuration, be denoted by  $\sigma$ . Then

$$\sigma = \llbracket p \rrbracket r_{in} = \mu_0 \left( \frac{r_{in}^2}{R_{in}^2} - \frac{R_{in}^2}{r_{in}^2} \right) h = \mu_0 \left( \frac{r_{in}}{R_{in}} - \frac{R_{in}^3}{r_{in}^3} \right) H, \tag{3.17}$$

where  $H$  equals the cylinder thickness in the undeformed configuration. With  $\tilde{\lambda} = r_{in}/R_{in}$ , we can write Eq. (3.17) as

$$\frac{\sigma}{H\mu_0} = \tilde{\lambda} - \frac{1}{\tilde{\lambda}^3} \tag{3.18}$$

implying that for a membrane composed of a homogeneous Mooney–Rivlin material the surface tension  $\sigma$  is a monotonically increasing function of the expansion ratio  $\tilde{\lambda}$ . We note that Eqs. (3.16) and (3.17) hold even when  $m \neq n$ .

For a cylinder subjected only to internal pressure  $p_{in}$ , Eq. (3.7) gives

$$-p_{in} = \frac{C_{10}}{R_{in}^m} \int_{r_{in}}^{r_{ou}} \frac{R^m}{r} \left( \frac{R^2}{r^2} - \frac{r^2}{R^2} \right) dr + \frac{C_{20}}{R_{in}^n} \int_{r_{in}}^{r_{ou}} \frac{R^n}{r} \left( \frac{r^2}{R^2} - \frac{R^2}{r^2} \right) dr, \tag{3.19}$$

for the determination of the constant  $A$ . When the cylinder is very thick,  $R_{ou} \gg R_{in}$ ,  $r_{ou} \rightarrow \infty$ , and Eq. (3.19) becomes

$$\frac{p_{in}}{A} = \frac{C_{10}}{R_{in}^m} \int_{R_{in}}^{\infty} \frac{A + 2R^2}{(A + R^2)^2} R^{m-1} dR + \frac{C_{20}}{R_{in}^n} \int_{R_{in}}^{\infty} \frac{A + 2R^2}{(A + R^2)^2} R^{n-1} dR. \tag{3.20}$$

For  $m = n$ , the hoop stress on the inner surface is given by

$$T_{\theta\theta}(r_{in}) = -p_{in} + \mu_0 \left( \frac{r_{in}^2}{R_{in}^2} - \frac{R_{in}^2}{r_{in}^2} \right) = -p_{in} + \frac{\mu_0 A}{R_{in}^2} \left( 1 + \frac{1}{A + R_{in}^2} \right). \tag{3.21}$$

The effect of the material inhomogeneity upon the stress concentration in a very thick cylinder made of a Mooney–Rivlin material appears in Eq. (3.21) through  $A$  that depends upon  $m$  and  $n$ ; cf. Eq. (3.20).

Before giving the expression for  $T_{rr}$  for arbitrary values of  $m$  and  $n$ , we provide it for  $m=n=\pm 1$  and  $\pm 2$ ; results for other integer values of  $m$  and  $n$  are listed in the Appendix. Stresses  $T_{\theta\theta}$  and  $T_{zz}$  can be computed from Eqs. (3.8)<sub>1</sub> and (3.8)<sub>2</sub>, respectively.

Case 1:  $m = 0, n = 0$ . For a cylinder composed of a homogeneous Mooney–Rivlin material, we get

$$\begin{aligned} T_{rr} &= \mu_0 \left[ \ln \frac{(r^2 - A)^{1/2}}{A} - \frac{A}{2r^2} \right] + K, \\ T_{\theta\theta} &= T_{rr} + \mu_0 \frac{A(-A + 2r^2)}{r^2(r^2 - A)}. \end{aligned} \tag{3.22}$$

Boundary conditions (2.4) imply that constants  $A$  and  $K$  are solutions of the following two non-linear equations:

$$\begin{aligned} \frac{p_{ou} - p_{in}}{\mu_0} &= \ln \frac{R_{in}}{R_{ou}} \left( \frac{A + R_{ou}^2}{A + R_{in}^2} \right)^{1/2} - \frac{A}{2} \frac{R_{ou}^2 - R_{in}^2}{(A + R_{ou}^2)(A + R_{in}^2)}, \\ K &= -p_{in} + \frac{A\mu_0}{2(A + R_{in}^2)} + \mu_0 \ln \frac{(A + R_{in}^2)^{1/2}}{R_{in}}. \end{aligned} \tag{3.23}$$

For given values of  $p_{in}, p_{ou}, R_{in}, R_{ou}$  and  $\mu_0$ , Eq. (3.23)<sub>1</sub> can be solved for  $A$ , and then  $K$  can be found from Eq. (3.23)<sub>2</sub>.

For a very thick cylinder subjected to internal pressure only,  $R_{ou} \gg R_{in}$ , Eq. (3.23)<sub>1</sub> becomes

$$\frac{2p_{in}}{\mu_0} = \ln \left( 1 + \frac{A}{R_{in}^2} \right) + \frac{A}{(A + R_{in}^2)}, \tag{3.24}$$

which still is a non-linear equation for the determination of  $A$ . In deriving Eq. (3.24) we have assumed that  $\lim_{R_{ou} \rightarrow \infty} (A/R_{ou}) = 0$ .

Case 2:  $m = n = 1$ .

$$\begin{aligned} T_{rr} &= \frac{\mu_0}{2R_{in}^2} \left[ 3\sqrt{A} \tan^{-1} \left( \frac{R}{\sqrt{A}} \right) - \frac{AR}{r^2} \right] + K, \\ T_{\theta\theta} &= T_{rr} + \frac{\mu_0}{R_{in}} \left( \frac{r^2}{R} - \frac{R^3}{r^2} \right). \end{aligned} \tag{3.25}$$

Equations for the determination of  $A$  and  $K$  from boundary conditions (2.4) are complicated, and are omitted. However, for given values of  $p_{in}, p_{ou}, R_{in}$  and  $R_{ou}$ , they can be solved numerically for  $A$  and  $K$ .

Case 3:  $m = n = 2$ .

$$T_{rr} = \frac{\mu_0}{2R_{in}^2} \left( \frac{A^2}{r^2} + 2A \ln r^2 \right) + K. \tag{3.26}$$

Constants  $A$  and  $K$  are solutions of the following two non-linear equations:

$$\begin{aligned} \frac{(p_{ou} - p_{in})R_{in}^2}{\mu_0} &= \frac{A^2(R_{ou}^2 - R_{in}^2)}{(A + R_{in}^2)(A + R_{ou}^2)} + A \ln \frac{A + R_{in}^2}{A + R_{ou}^2}, \\ K &= - \left[ p_{in} + \frac{\mu_0}{2R_{in}^2} + \left( \frac{A^2}{A + R_{in}^2} 2A \ln(A + R_{in}^2) \right) \right]. \end{aligned} \tag{3.27}$$

Case 4:  $m = n = -1$ .

$$T_{rr} = -\mu_0 R_{in} \left[ \frac{1}{R} - \frac{R}{2r^2} + \frac{1}{2\sqrt{A}} \tan^{-1} \left( \frac{R}{\sqrt{A}} \right) \right] + K. \tag{3.28}$$

Case 5:  $m = n = -2$ .

$$T_{rr} = -\frac{\mu_0 A R_{in}^2}{2r^2(r^2 - A)} + K, \\ T_{\theta\theta} = T_{rr} + \mu_0 \frac{R_{in}^2 r^2}{(r^2 - A)^2}. \tag{3.29}$$

Constants  $A$  and  $K$  are solutions of the following two equations obtained from boundary conditions (2.4):

$$A^2 + A(R_{in}^2 + R_{ou}^2) + R_{in}^2 R_{ou}^2 (1 - \hat{\alpha}) = 0, \\ \hat{\alpha} = 1 / \left( 1 + \frac{2(p_{ou} - p_{in})R_{ou}^2}{\mu_0 (R_{ou}^2 - R_{in}^2)} \right) \\ K = \frac{\mu_0}{2} \left( \frac{A}{A + R_{in}^2} \right) - p_{in}. \tag{3.30}$$

For a very thick cylinder subjected to internal pressure only, Eqs. (3.30) become

$$\hat{\alpha} = \frac{\mu_0}{\mu_0 - 2p_{in}}, \\ A = 2R_{in}^2 p_{in} / (\mu_0 - 2p_{in}). \tag{3.31}$$

The requirement  $A > 0$  restricts  $p_{in}$  to be less than  $\mu_0/2$ . Thus

$$T_{\theta\theta}(r_{in}) = -p_{in} + \frac{\mu_0^2}{\mu_0 - 2p_{in}}. \tag{3.32}$$

We have also studied problems involving unequal integer values of  $m$  and  $n$ ; some of these results are discussed in Section 4.

### 3.1.2. FG cylinder with arbitrary values of $m, n$ , and $D$

We first assume that  $m \neq 0, n \neq 0, m + 2 \neq 0, n + 2 \neq 0$ , and note that

$$\int \left( \frac{r^2}{D^2 R^2} - \frac{R^2}{r^2} \right) \frac{R^n}{r} dr = \int R^{n-2} r dr - \int \frac{R^{n+2}}{r^3} dr, \\ = \frac{1}{D} \int R^{n-1} dR - D \int \frac{R^{n+3}}{(A + DR^2)^2}, \\ = \frac{1}{D} \frac{R^n}{n} - \frac{R^{n+2}}{A(n+2)} \left[ {}_2F_1 \left( \frac{n}{2} + 1, 1; \frac{n}{2} + 2; -\frac{DR^2}{A} \right) \right. \\ \left. - {}_2F_1 \left( \frac{n}{2} + 1, 2; \frac{n}{2} + 2; -\frac{DR^2}{A} \right) \right], \tag{3.33}$$

where  ${}_2F_1(a, b; c; x)$  is the Gauss hypergeometric function [16]. Similarly

$$\int \left( \frac{D^2 R^2}{r^2} - \frac{r^2}{R^2} \right) \frac{R^m}{r} dr = D^3 \int \frac{R^{m+3}}{(A + DR^2)^2} dR - D \int R^{m-1} dR \\ = \frac{D^2 R^{m+2}}{A(m+2)} \left[ {}_2F_1 \left( \frac{m}{2} + 1, 1; \frac{m}{2} + 2; -\frac{DR^2}{A} \right) \right. \\ \left. - {}_2F_1 \left( \frac{m}{2} + 1, 2; \frac{m}{2} + 2; -\frac{DR^2}{A} \right) \right] - \frac{DR^m}{m}. \tag{3.34}$$

Eqs. (3.33), (3.34) and (3.7) give

$$T_{rr} = -p_{in} + \frac{C_{10}}{R_{in}^m} \left[ \frac{DR^m}{m} - \frac{D^2 R^{m+2}}{A(m+2)} \left( {}_2F_1 \left( \frac{m}{2} + 1, 1; \frac{m}{2} + 2; -\frac{DR^2}{A} \right) \right. \right. \\ \left. \left. + {}_2F_1 \left( \frac{m}{2} + 1, 2; \frac{m}{2} + 2; -\frac{DR^2}{A} \right) \right) \right]_{r_{in}}^r \\ + \frac{C_{20}}{R_{in}^n} \left[ -\frac{R^n}{Dn} + \frac{R^{n+2}}{A(n+2)} \left( {}_2F_1 \left( \frac{n}{2} + 1, 1; \frac{n}{2} + 2; -\frac{DR^2}{A} \right) \right. \right. \\ \left. \left. - {}_2F_1 \left( \frac{n}{2} + 1, 2; \frac{n}{2} + 2; -\frac{DR^2}{A} \right) \right) \right]_{r_{in}}^r. \tag{3.35}$$

The constant  $A$  is found from the boundary condition  $T_{rr}(r_{ou}) = -p_{ou}$ . Knowing  $T_{rr}, T_{\theta\theta}$  and  $T_{zz}$  are determined from Eqs. (3.8)<sub>1</sub> and (3.8)<sub>2</sub>.

For a cylinder composed of a homogeneous Mooney–Rivlin material,  $m = n = 0$ ,  $T_{rr}$  and  $T_{\theta\theta}$  are given by

$$T_{rr} = -\frac{\mu_1}{D} \left( \ln \frac{r}{R} + \frac{A}{2r^2} \right) + K, \\ T_{\theta\theta} = T_{rr} + \mu_1 \left( \frac{r^2}{D^2 R^2} - \frac{R^2}{r^2} \right), \tag{3.36}$$

and for  $m + 2 = n + 2 = 0$ , we have

$$T_{rr} = \mu_1 \frac{R_{in}^2}{2} \left( \frac{1}{r^2} - \frac{1}{DR^2} \right) + K, \\ T_{\theta\theta} = T_{rr} + \mu_1 \frac{R_{in}^2 r^2}{DR^2} + K, \tag{3.37}$$

where

$$\mu_1 = D^2 C_{10} - C_{20}.$$

For  $D = 1$ , Eqs. (3.36) and (3.37) reduce to Eqs. (3.22) and (3.29), respectively.

### 3.2. Affine variation of $C_1(R)$ and $C_2(R)$

We now consider the case when  $C_1$  and  $C_2$  are affine functions of the radius  $R$ . That is

$$C_1 = \hat{C}_{10} \left( 1 + \alpha \frac{R}{R_{in}} \right), \quad C_2 = \hat{C}_{20} \left( 1 + \beta \frac{R}{R_{in}} \right), \tag{3.38}$$

where  $\alpha$  and  $\beta$  are real numbers. The normal stresses are given by

$$\frac{1}{D} T_{rr} = \hat{C}_{10} \left[ \frac{3}{2} \sqrt{\frac{A}{D}} \frac{\alpha}{R_{in}} \tan^{-1} \left( \sqrt{\frac{D}{A}} R \right) - \ln \frac{\sqrt{A + DR^2}}{R} - \frac{A(1 + \alpha R/R_{in})}{2(A + DR^2)} \right] \\ - \hat{C}_{20} \left[ \frac{3}{2} \sqrt{\frac{A}{D^5}} \frac{\beta}{R_{in}} \tan^{-1} \left( \sqrt{\frac{D}{A}} R \right) - \frac{1}{D^2} \ln \frac{\sqrt{A + DR^2}}{R} \right. \\ \left. - \frac{A(1 + \beta R/R_{in})}{2D^2(A + DR^2)} \right] + K,$$

$$T_{\theta\theta} = T_{rr} + \hat{C}_{10} \left( 1 + \alpha \frac{R}{R_{in}} \right) \left( \frac{r^2}{R^2} - \frac{D^2 R^2}{r^2} \right) \\ + \hat{C}_{20} \left( 1 + \beta \frac{R}{R_{in}} \right) \left( \frac{R^2}{r^2} - \frac{r^2}{D^2 R^2} \right),$$

$$T_{zz} = T_{rr} + \hat{C}_{10} \left(1 + \alpha \frac{R}{R_{in}}\right) \left(\frac{1}{D^2} - \frac{D^2 R^2}{r^2}\right) + \hat{C}_{20} \left(1 + \beta \frac{R}{R_{in}}\right) \left(D^2 - \frac{r^2}{D^2 R^2}\right). \quad (3.39)$$

For  $\alpha = \beta$ , and plane strain axisymmetric deformations, (i.e.,  $D = 1$ ), Eqs. (3.39)<sub>1</sub>–(3.39)<sub>3</sub> simplify to the following:

$$T_{rr} = \hat{\mu}_0 \left[ \frac{3}{2} \frac{\sqrt{A}\alpha}{R_{in}} \tan^{-1} \left[ \frac{R}{\sqrt{A}} \right] - \ln \frac{\sqrt{A+R^2}}{R} - \frac{A(1+\alpha R/R_{in})}{2(A+R^2)} \right] + K,$$

$$T_{\theta\theta} = T_{rr} + \hat{\mu}_0 \left(1 + \alpha \frac{R}{R_{in}}\right) \left(\frac{r^2}{R^2} - \frac{R^2}{r^2}\right),$$

$$T_{zz} = T_{rr} + \left(1 + \alpha \frac{R}{R_{in}}\right) \left(\hat{C}_{10} - \frac{\hat{C}_{20} R^2}{R^2}\right) \left(1 - \frac{R^2}{r^2}\right), \quad (3.40)$$

where

$$\hat{\mu}_0 = \hat{C}_{10} - \hat{C}_{20}. \quad (3.41)$$

For radial expansion of the cylinder, the term  $(r^2/R^2 - R^2/r^2) > 0$ . Thus  $T_{\theta\theta} > T_{rr}$  for  $-R_{in}/R_{ou} > \alpha > 0$ , and for  $\alpha R_{ou}/R_{in} < -1$ ,  $T_{\theta\theta} < T_{rr}$  provided that  $\hat{\mu}_0 > 0$ .

### 4. Numerical results

During the computation of numerical results we set

$$C_{10} = \hat{C}_{10} = 1.858 \times 10^5 \text{ Pa}, \quad C_{20} = \hat{C}_{20} = -0.1935 \times 10^5 \text{ Pa},$$

$$R_{in} = 1 \text{ m}, \quad p_{in} = 0.01 C_{10},$$

and  $R_{ou}/R_{in} = 10$ . These values of  $C_{10}$  and  $C_{20}$  are for the rubber tested by Batra et al. [19]. When studying stress concentration on the inner surface of a very thick cylinder we take  $R_{ou}/R_{in} = 100$ . However, while delineating surface tension in a very thin cylinder,

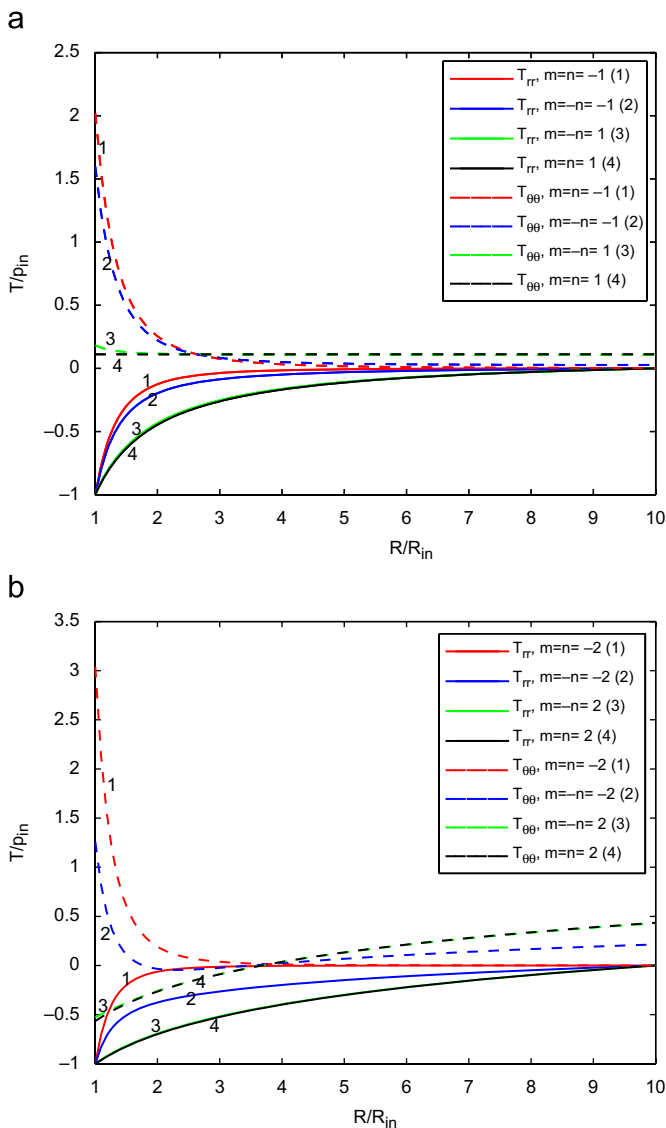


Fig. 1. For  $R_{ou}/R_{in} = 10$  and  $p_{ou} = 0$ , through-the-thickness distributions of the normalized radial stress and the normalized hoop stress for (a)  $m = \pm n = \pm 1$  and (b)  $m = \pm n = \pm 2$ .

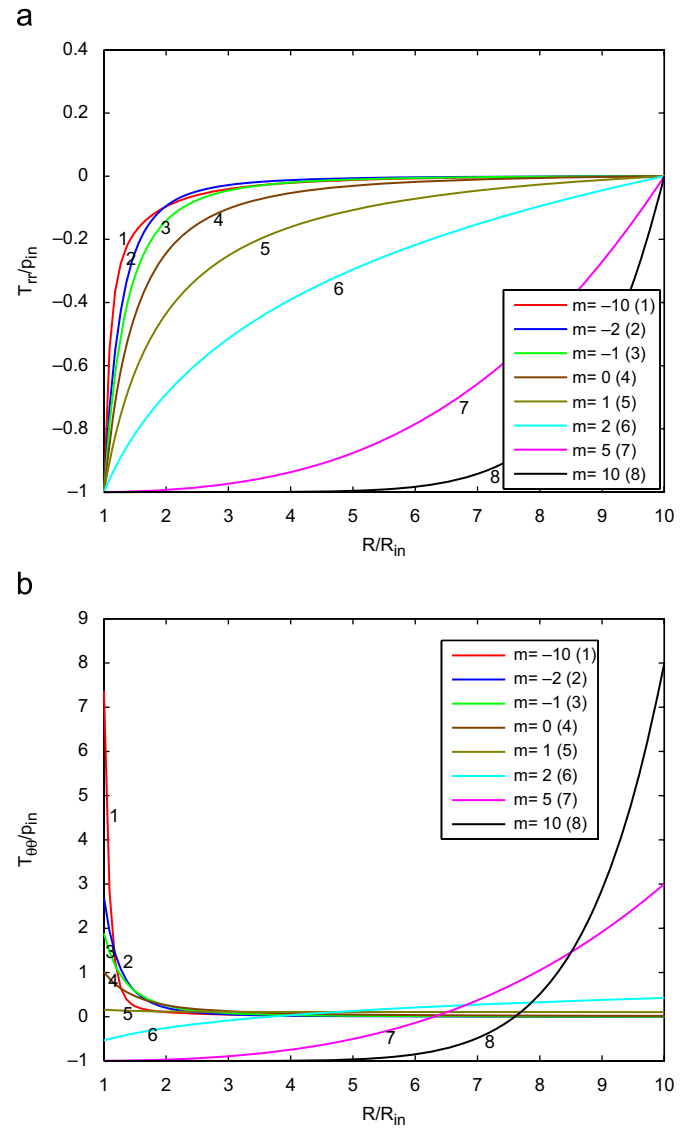
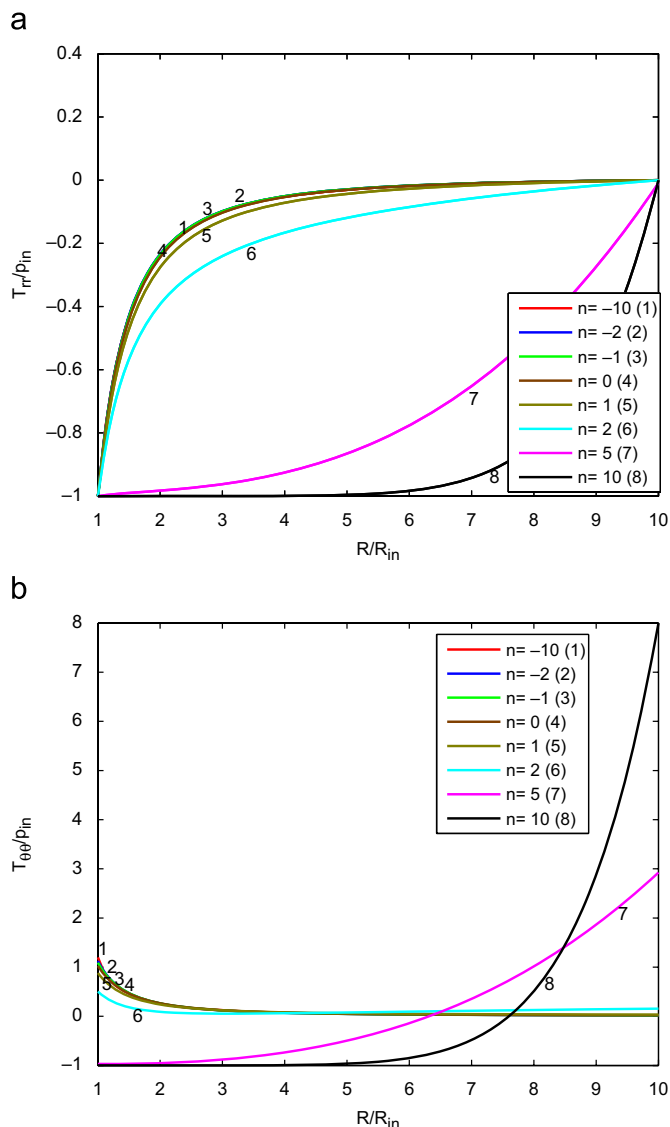


Fig. 2. For  $R_{ou}/R_{in} = 10$ ,  $p_{ou} = 0$ , and  $n = 0$ ,  $m = -10, -2, -1, 0, 1, 2, 5, 10$ , through-the-thickness distributions of (a) the normalized radial stress and (b) the normalized hoop stress.



**Fig. 3.** For  $R_{ou}/R_{in} = 10$ ,  $p_{ou} = 0$ , and  $m = 0$ ,  $n = -10, -2, -1, 0, 1, 2, 5, 10$ , through-the-thickness distributions of (a) the normalized radial stress and (b) the normalized hoop stress.

we set  $R_{ou}/R_{in} = 1.01$  and  $1.001$ . For  $R_{ou}/R_{in} = 1.001$ , we compute results for  $p_{in} = 0.001C_{10}$ .

#### 4.1. Inflation of a FG cylinder

##### 4.1.1. Power law variation of $C_1$ and $C_2$

**4.1.1.1. Pressure applied on the inner surface.** For  $m = \pm n = \pm 1$  (four cases) and  $m = \pm n = \pm 2$ , we have plotted in Fig. 1a and b the through-the-thickness variation of  $T_{rr}/p_{in}$  and  $T_{\theta\theta}/p_{in}$  for a cylinder loaded by internal pressure only. The Cauchy stresses are plotted against the radius in the undeformed configuration since  $r_{in}$  and  $r_{ou}$  depend upon values of  $m$  and  $n$ , and one will not have the same range of values of  $r$  for different values of  $m$  and  $n$ . For  $m = \pm n = \pm 1$  magnitudes of  $T_{rr}$  and  $T_{\theta\theta}$  are the maximum at points on the inner surface of the cylinder. For  $m = n = 1$ , the elasticities  $C_{10}$  and  $C_{20}$  increase linearly with the radius  $R$  in the reference configuration. That is, the material hardens as one moves outwards from the inner surface. For this case, it is interesting to note that  $T_{\theta\theta}$  is nearly uniform throughout the cylinder thickness; e.g. see the dashed curve 4

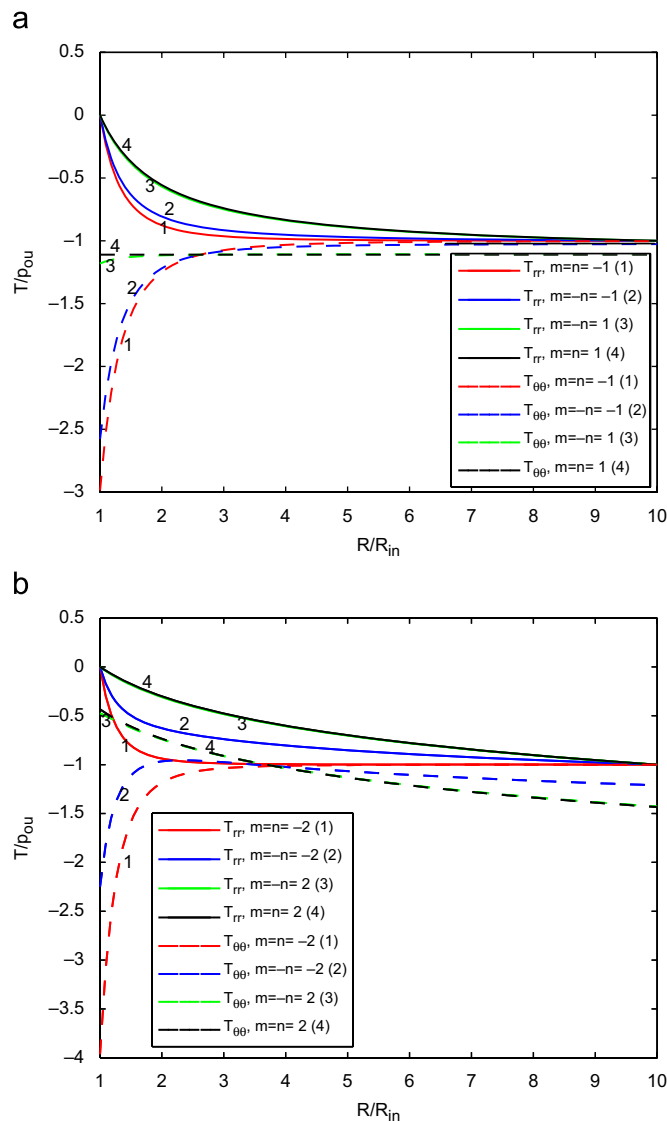


**Fig. 4.** For  $R_{ou}/R_{in} = 10$  and  $p_{in} = 0$ , through-the-thickness distributions of the normalized radial stress and the normalized hoop stress for (a)  $m = \pm n = \pm 1$  and (b)  $m = \pm n = \pm 2$ .

in Fig. 1a. For a cylinder composed of an incompressible Hookean material it was proved in [6,8] that  $T_{\theta\theta}$  is a constant when the shear modulus is a linear function of the radius  $R$ . However, for a compressible Hookean material studied in [11] the hoop stress is not uniform through the cylinder thickness for a linear variation of Young's modulus.

For a cylinder comprised of an incompressible second-order elastic material it was found in [6] that  $T_{\theta\theta}$  is not uniform through the cylinder thickness when the two elasticities,  $\mu$  and  $\alpha$ , in

$$\mathbf{T} = -p\mathbf{1} + \mu(\mathbf{H} + \mathbf{H}^T + \mathbf{H}\mathbf{H}^T) + \alpha(\mathbf{H} + \mathbf{H}^T)^2, \quad (4.1)$$

are linear functions of  $R$ . Here  $\mathbf{H} = \mathbf{F} - \mathbf{1}$  equals the displacement gradient. The admissible radial displacement field,  $u$ , in [6] was found to be

$$u = \frac{\tilde{A}}{R} - \frac{\tilde{B}}{R^3}, \quad (4.2)$$

where constants  $\tilde{A}$  and  $\tilde{B}$  are, respectively, linear and quadratic functions of the applied pressure. Setting  $\mathbf{F} = \mathbf{I} + \mathbf{H}$  in Eq. (2.1) and keeping

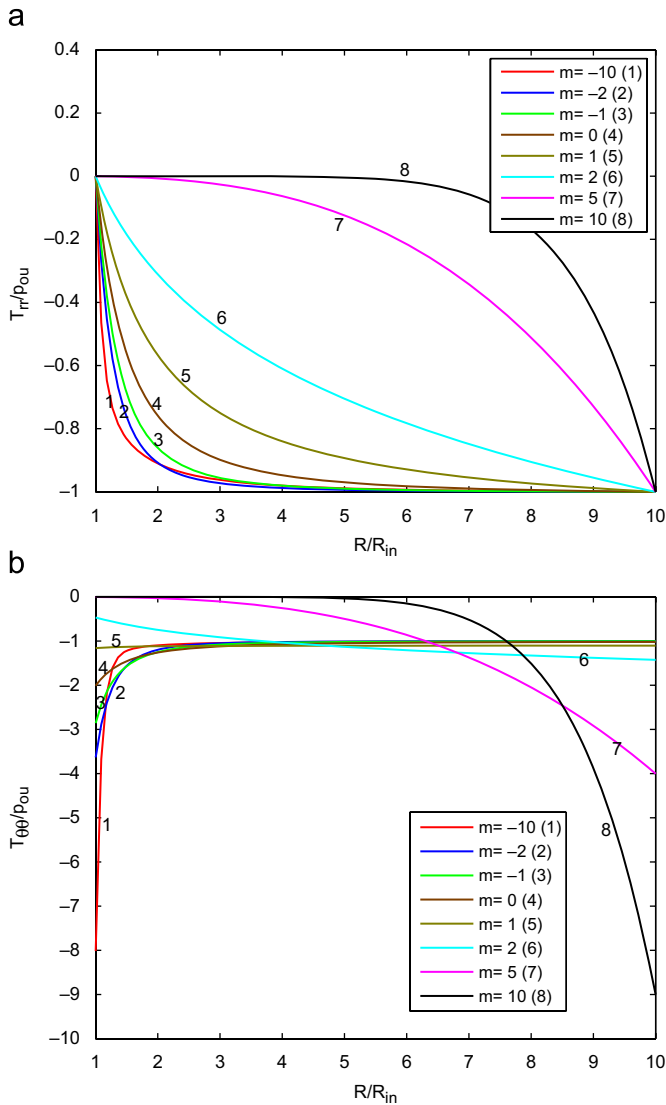


**Fig. 5.** For  $R_{ou}/R_{in} = 10$ ,  $p_{in} = 0$ , and  $n = 0$ ,  $m = -10, -2, -1, 0, 1, 2, 5, 10$ , through-the-thickness distributions of (a) the normalized radial stress and (b) the normalized hoop stress.

second-order terms in  $\mathbf{H}$  gives

$$\mathbf{T} = -p\mathbf{1} + (C_1 - C_2)(\mathbf{H} + \mathbf{H}^T + \mathbf{H}\mathbf{H}^T) + C_2(\mathbf{H} + \mathbf{H}^T)^2, \quad (4.3)$$

which is the same as Eq. (4.1) when  $\mu = (C_1 - C_2)$ , and  $\alpha = C_2$ .

Setting  $D = 1$ , and  $r = R + \varepsilon u^{(1)} + \varepsilon^2 u^{(2)}$ ,  $A = \varepsilon A^{(1)} + \varepsilon^2 A^{(2)}$  in Eq. (3.3)<sub>1</sub> gives Eq. (4.2) for the displacement field for an incompressible isotropic second-order elastic material. Here  $\varepsilon \ll 1$ , and  $A^{(1)}$  and  $A^{(2)}$  are constants. However, we are unable to find constants  $A^{(1)}$  and  $A^{(2)}$  from Eq. (3.9) since  $g_1$  is a complicated function of  $A$ .

For  $m=n=-2$  the magnitude of the radial stress decreases rapidly from  $p_{in}$  on the inner surface of the cylinder to almost zero at points where  $R/R_{in} = 2$ ; see the solid curve 1 in Fig. 1b. The hoop stress for  $m=n=-2$  is also high in this boundary-layer region. Whereas  $T_{\theta\theta}(R_{in})$  is tensile for  $m=n=-2$  and  $m=-n=-2$ , it is compressive for  $m=-n=2$  and  $m=n=2$ . The through-the-thickness variations of  $T_{rr}$  and  $T_{\theta\theta}$  for  $m=n=2$  and  $m=-n=2$  (i.e., curves 3 and 4 in Fig. 1b) are nearly coincident. Thus the sign and the magnitude of the hoop stress on the inner surface strongly depend upon the values of  $m$  and  $n$ .

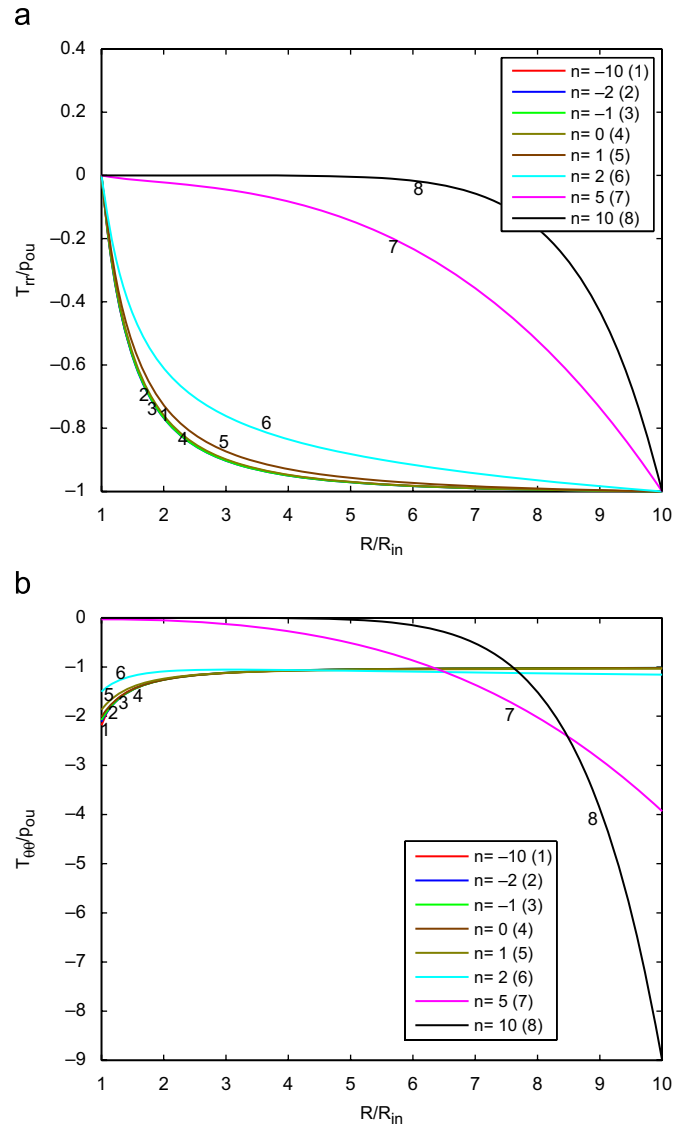


**Fig. 6.** For  $R_{ou}/R_{in} = 10$ ,  $p_{in} = 0$ , and  $m = 0$ ,  $n = -10, -2, -1, 0, 1, 2, 5, 10$ , through-the-thickness distributions of (a) the normalized radial stress and (b) the normalized hoop stress.

Numerical results were also computed for  $m = \pm n = \pm 5$  and  $\pm 10$  but are not shown here for the sake of brevity. However, we describe a few features of these results. The thickness of the boundary layer in Fig. 1b for  $m=n=-2$  decreases further to  $0.3R_{in}$  for  $m=n=-10$ . Whereas the hoop stress at points near the inner surface of the cylinder is tensile for  $m=n=-1$  (dashed curve 1 in Fig. 1a), it is compressive for  $m=n=2$  (dashed curve 4 in Fig. 1b),  $m=-n=5$ ,  $m=n=5$  and  $m=n=-10$ . For  $m=n=10$ , the hoop stress and the radial stress are compressive and equal nearly  $p_{in}$  for  $R_{in} \leq R \leq 5R_{in}$ ; however, their magnitudes equal, respectively, zero and  $8p_{in}$  on the outer surface  $R = R_{ou} = 10R_{in}$ . Hence through-the-thickness variation of stresses can be dramatically altered by suitably grading the elastic parameters  $C_1$  and  $C_2$ .

For  $n = 0$  and different values of  $m$ , Fig. 2a and b exhibits through-the-thickness variations of  $T_{rr}/p_{in}$  and  $T_{\theta\theta}/p_{in}$  for an internally loaded thick cylinder. Results for a cylinder composed of a homogeneous material correspond to  $m=n=0$ . For  $m=-10, -2, -1, 1$  and  $2$  the distribution of the radial stress in the cylinder wall is qualitatively similar to that in a cylinder composed of a

**Table 1**  
For different values of  $m$  and  $n$ , the hoop stress at the inner and the outer surfaces of an internally pressurized FG cylinder.

$m$	$n$	$T_{\theta\theta}(R_{in})/p_{in}$	$T_{\theta\theta}(R_{ou})/p_{in}$
-10	0	7.3358577	0.000080108
-2	0	2.6833819	0.000035065
-1	0	1.87920980	0.0000299587
0	0	1.00476505	0.0002013863
1	0	0.059661719	0.0096301738
5	0	-0.99999668	3.0000025314
10	0	-0.99999999	8.000000000
0	-10	1.17640223	0.000198083
0	-2	1.10446762	0.000191507
0	-1	1.07017190	0.000188565
0	1	0.83410685	0.001903936
0	2	0.12697982	0.106671662
0	5	-0.99996819	2.99995979
0	10	-0.99999999	7.99999999
-1	-1	2.01650849	0
-1	1	1.538883307	0.002410782
1	-1	0.077613245	0.009783626
1	1	0.010126479	0.010124365
-2	-2	3.0368995501	0
-2	2	0.512832756	0.143180973
2	-2	-0.76167153	0.2159655001
2	2	-0.78292469	0.217181990
5	5	-0.99999699	3.00000300
5	-5	-0.99999668	3.00000286
-5	5	-0.99996819	2.99999065
-5	-5	6.15366193	0
10	10	-1	8
10	-10	-1	8
-10	-10	11.55154263	0
-10	10	-1	8

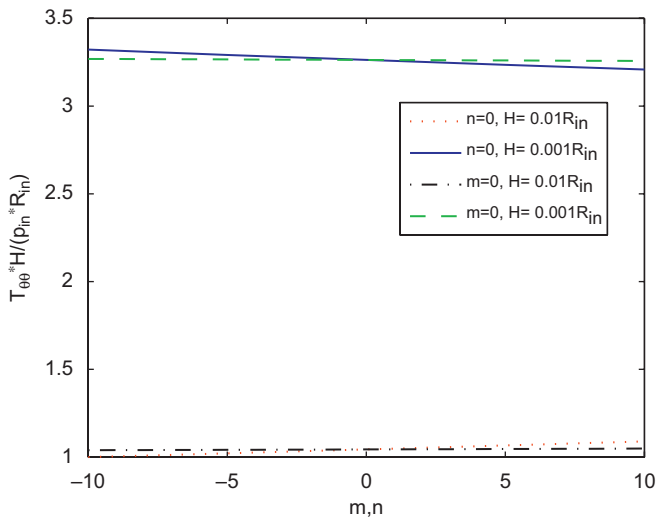


**Fig. 7.** The normalized hoop stress at  $R=R_m$  for different values of  $m$  and  $n$  for thin cylinder ( $R_{ou}/R_{in} = 1.01, 1.001$ ).

homogeneous Mooney–Rivlin material. However, for  $m = 5$  and  $10$ , the curvature of the  $T_{rr}$  vs.  $R$  curve (curves 7 and 8 in Fig. 2a) is opposite to that of the curves for other values of  $m$  considered here. For  $m = 10$ ,  $T_{rr} = T_{\theta\theta} \sim -p_{in}$  for  $R_{in} \leq R \leq 5R_{in}$ . For  $m = -10$  the hoop stress, as indicated by curve 1 in Fig. 2b, is concentrated in the region  $R_{in} \leq R \leq 1.3R_{in}$ , and  $T_{\theta\theta}(r_{in}) \simeq 7.5p_{in}$ . For  $m = 1$ ,  $T_{\theta\theta}(r)$  equals  $\sim 0.15p_{in}$  throughout the cylinder thickness; e.g. see curve 5 in Fig. 2b. The curvature of the curve  $T_{\theta\theta}$  vs.  $R$  for  $m = 2$  is different from that for other values of  $m$ , and through-the-thickness variations of  $T_{\theta\theta}$  for  $m = 5$  and  $10$  differ quantitatively and qualitatively from

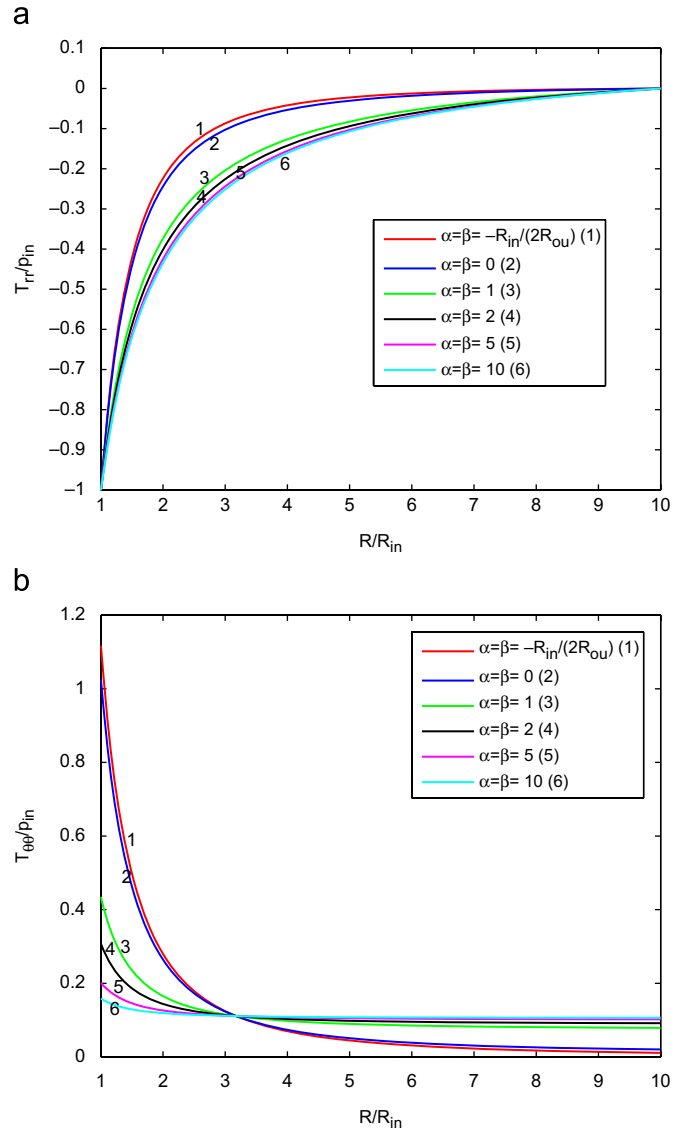


**Fig. 8.** For  $R_{ou}/R_{in} = 10$ ,  $p_{ou} = 0$ , and  $\alpha = \beta = -R_{in}/(2R_{ou})$ , 0, 1, 2, 5, 10, through-the-thickness distributions of (a) the normalized radial stress and (b) the normalized hoop stress.

those for other values of  $m$ . For  $m = 5$  and  $10$ , the maximum tensile hoop stress occurs on the outer surface of the cylinder, and equals  $\sim 3p_{in}$  and  $\sim 7.8p_{in}$ , respectively. Whereas the tensile hoop stress is maximum on the inner surface for  $m = -10$ , it is maximum at the outersurface for  $m = 10$ , and their magnitudes are nearly equal.

Through-the-thickness distributions of  $T_{rr}$  and  $T_{\theta\theta}$  for  $m = 0$  and different values of  $n$  are exhibited in Fig. 3a and b. Whereas the variations of  $T_{rr}$  with  $R$  for  $m = 0$  and  $n \neq 0$  are qualitatively similar to those of  $T_{rr}$  with  $R$  for  $n = 0$  and  $m \neq 0$ , those of  $T_{\theta\theta}$  vs.  $R$  for the two cases are quite different. Results plotted in Fig. 3a and b are essentially the same for  $n = -10, -2, -1$  and  $0$ ; those for  $n = 1$  and  $2$  are qualitatively similar to the ones for  $n = 0$ , i.e., the cylinder composed of a homogeneous Mooney–Rivlin material. However, through-the-thickness variations of  $T_{rr}$  and  $T_{\theta\theta}$ , as indicated by curves 7 and 8, for  $n = 5$  and  $10$  are remarkably different from those for  $n = 0$  with  $T_{\theta\theta}$  being tensile in the cylinder material near the outer surface. For  $n = 5$  and  $10$ ,  $T_{\theta\theta}(R_{ou})/p_{in}$  equal  $\sim 2.85$  and  $\sim 7.9$ , respectively. Thus if the cylinder material were to fail because of the maximum principal tensile stress exceeding a critical value, the gradation of material

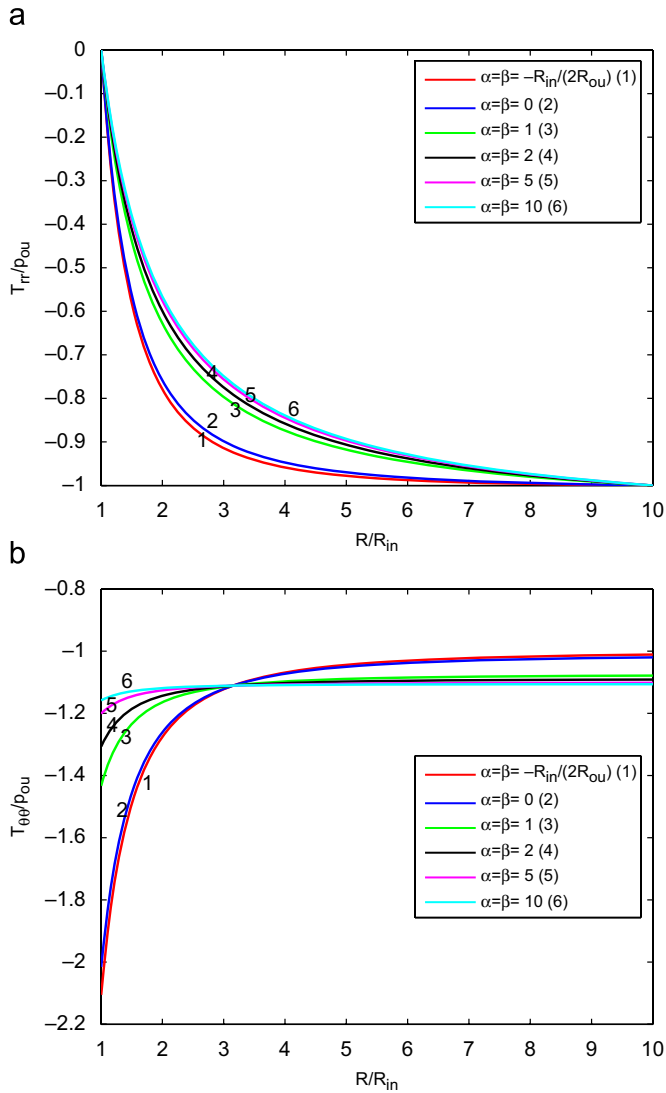


Fig. 9. For  $R_{ou}/R_{in}=10$ ,  $p_{in}=0$ , and  $\alpha=\beta=-R_{in}/(2R_{ou})$ , 0, 1, 2, 5, 10, through-the-thickness distributions of (a) the normalized radial stress and (b) the normalized hoop stress.

properties will determine whether the failure occurs on the inner surface or on the outer surface.

4.1.1.2. Pressure applied on the outer surface. For a thick cylinder loaded by a pressure,  $p_{ou} = 0.01C_{10}$ , on the outer surface, through-the-thickness variations of  $T_{rr}$  and  $T_{\theta\theta}$  for different values of  $m$  and  $n$  are plotted in Figs. 4a,b, 5a,b and 6a,b. For  $n = 0$  and  $m = 1$ , the hoop stress is essentially uniform through the cylinder thickness. However, for  $m = 0$  and all integer values of  $n$  considered the hoop stress is non-uniform through the cylinder thickness. For  $(n, m)$  equal to (0, 5), (0, 10), (5, 0) and (10, 0) the maximum compressive hoop stress occurs on the outer surface and its magnitude equals 4, 9, 3.8 and 10, respectively; for other values of  $m$  and  $n$  studied the magnitude of the compressive hoop stress is maximum at a point on the inner surface of the cylinder.

4.1.1.3. Cylinder with  $R_{ou}/R_{in} = 100$ . For either  $m = 0$  or  $n = 0$  and values of  $n$  and  $m$  the same as those considered above, the qualitative variation of  $T_{rr}$  and  $T_{\theta\theta}$  through the cylinder thickness for an internally pressurized cylinder is unaltered even when the ratio of the outer radius to the inner radius in the undeformed

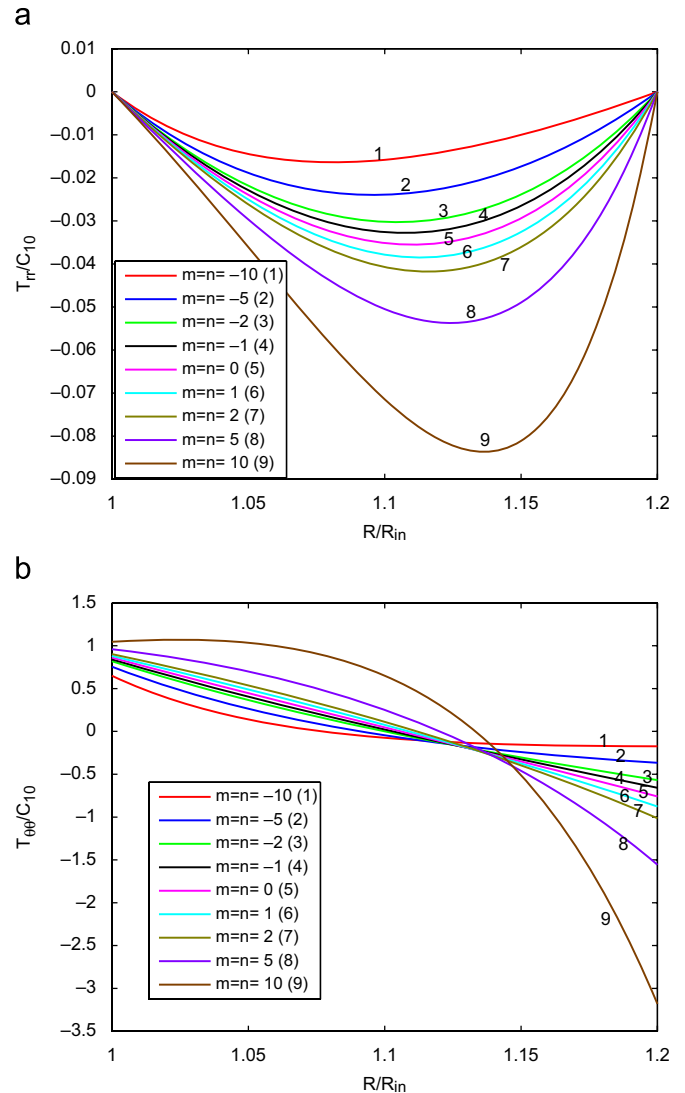


Fig. 10. For eversion of a cylinder with  $R_{ou}/R_{in} = 1.2$ , and  $m=n=0, \pm 1, \pm 2, \pm 5, \pm 10$ , through-the-thickness distributions of (a) the normalized radial stress and (b) the normalized hoop stress.

configuration is increased from 10 to 100. Thus results are summarized in Table 1. It is clear from the values listed in Table 1 that, in a FG very thick cylinder with pressure applied only to the inner surface, the maximum tensile hoop stress at the outer surface can be very large; this result is counter-intuitive.

4.1.1.4. Cylinder with  $R_{ou}/R_{in} = 1.01, 1.001$ . For a thin cylinder with  $R_{ou}/R_{in} = 1.01$  and loaded internally,  $T_{\theta\theta}/p_{in}$  varies through the cylinder thickness, and decreases nearly affinely from its maximum value on the inner surface to the minimum value on the outer surface, except for  $m = 0$  and  $n = 5, 10$ . For these two cases,  $T_{\theta\theta}/p_{in}$  increases affinely from its minimum value on the inner surface to its maximum value on the outer surface. For either  $m=0$  or  $n=0$ , Fig. 7a and b exhibits the variation with  $n$  and  $m$  of  $(HT_{\theta\theta}(R_{in})) / (p_{in}R_{in})$  on the assumption that  $T_{\theta\theta}(R_{in})$  is a continuous function of  $m$  and  $n$ . Thus the hoop stress in a thin cylinder can be controlled by suitably grading the material properties. Here  $H = (R_{ou} - R_{in})$  equals the cylinder thickness in the reference configuration. We note that a thin cylinder has not been approximated as a membrane, thus stresses induced in it depend upon values assigned to exponents  $m$  and  $n$ .

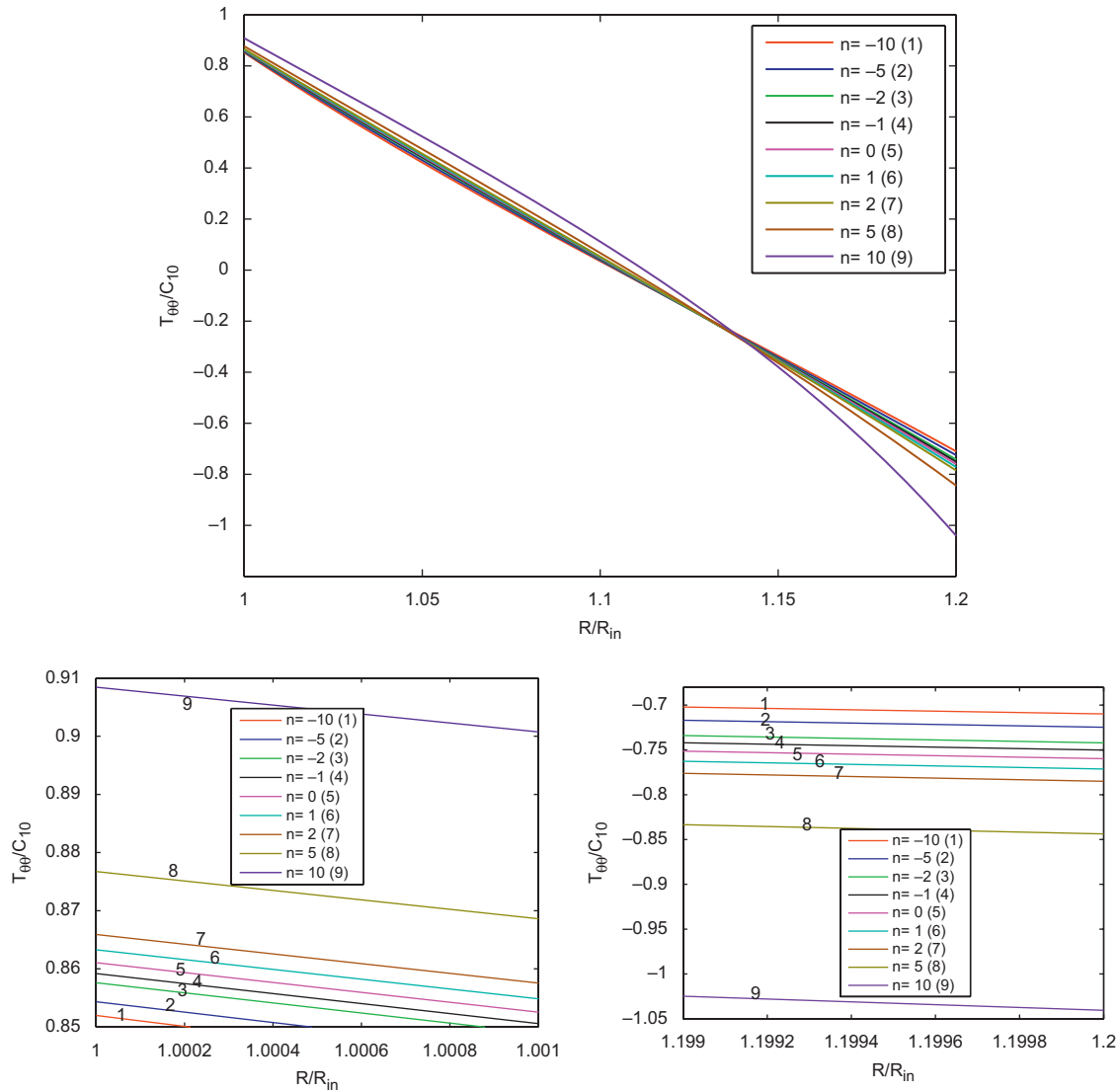


Fig. 11. For eversion of a cylinder with  $R_{ou}/R_{in} = 1.2$ , and  $m = 0, n = 0, \pm 1, \pm 2, \pm 5, \pm 10$ , through-the-thickness distributions of the normalized hoop stress.

#### 4.1.2. Affine variation of $C_1$ and $C_2$

For an internally pressured cylinder Fig. 8a and b shows the through-the-thickness variation of the radial and the hoop stresses for different values of  $\alpha = \beta$ . It is clear that values of  $\alpha$  and  $\beta$  have a little effect on the variation of  $T_{rr}$  but influence noticeably the through-the-thickness distribution of the hoop stress. It is interesting to note that  $T_{\theta\theta}$  at the point  $R = \sqrt{R_{in}R_{ou}} = 3.16$  is essentially unchanged by the values of  $\alpha$  and  $\beta$ , and is the same as that in the cylinder made of a homogeneous material. For an FG cylinder composed of an incompressible Hookean material with the affine variation of the shear modulus, one can prove analytically that the hoop stress at  $R = \sqrt{R_{in}R_{ou}}$  is the same for all affine variations of the shear modulus. However, for the FG cylinder made of a Mooney–Rivlin material, computed values of  $T_{\theta\theta}(\sqrt{R_{in}R_{ou}})$  are the same but we cannot prove the result analytically.

In a FG cylinder subjected to pressure on the external surface only, through-the-thickness variations of stresses plotted in Fig. 9a and b evince that both  $T_{rr}$  and  $T_{\theta\theta}$  are compressive throughout the cylinder, and the maximum magnitude of  $T_{\theta\theta}$  occurs at points on the inner surface of the cylinder. For a cylinder with  $R_{ou} = 10R_{in}$ ,  $T_{\theta\theta}$  varies noticeably with the values of  $\alpha$  and  $\beta$  only in the region

$R_{in} \leq R \leq 3R_{in}$ . At  $R = \sqrt{R_{in}R_{ou}} = 3.16$ ,  $|T_{\theta\theta}|$  is nearly independent of the equal values assigned to  $\alpha$  and  $\beta$ .

#### 4.2. Eversion of a FG cylinder

##### 4.2.1. Power law variation of $C_1(R)$ and $C_2(R)$

We find stresses induced during the eversion of a circular cylindrical tube by setting  $p_{ou} = p_{in} = 0$  and  $F_a = 0$  in Eqs. (3.91)<sub>1</sub> and (3.91)<sub>2</sub>, respectively. The resulting two equations are solved for constants  $A$  and  $D$ . Note that  $A$  must be negative for the eversion problem.

For  $R_{ou}/R_{in} = 1.2$  and different values of  $m = n$ , we have plotted in Fig. 10a and b through-the-thickness variations of the radial and the hoop stresses. The abscissa in these plots represents the radial coordinate in the unstressed reference configuration. For all values of  $m = n$  considered, the hoop stress is tensile on the inner surface of the everted tube and compressive on the outer surface. For  $m = n = 10$  and  $-10$ , the maximum magnitude of the hoop stress equals  $\sim 3.2C_{10}$  and  $\sim 0.2C_{10}$ . The radial stress is everywhere compressive and the maximum magnitude of  $T_{rr}$  is very small as compared to that of  $T_{\theta\theta}$ .

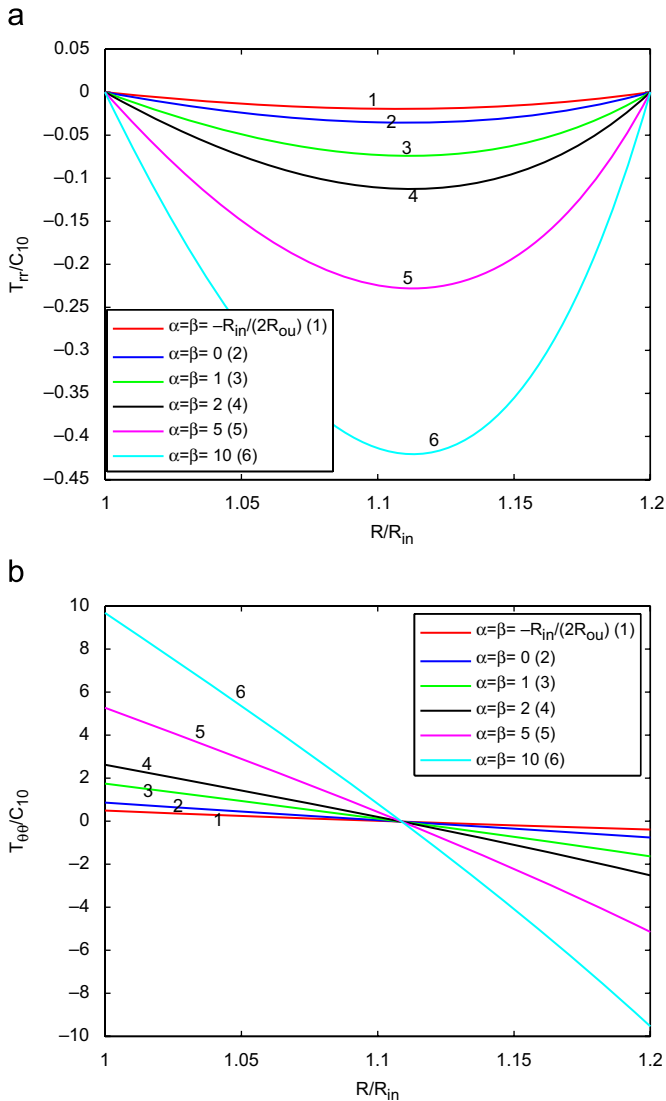


Fig. 12. For eversion of a cylinder with  $R_{ou}/R_{in} = 1.2$ , and  $\alpha = \beta = -R_{in}/(2R_{ou})$ , 0, 1, 2, 5, 10, through-the-thickness distributions of (a) the normalized radial stress and (b) the normalized hoop stress.

The point where  $|T_{rr}|$  is maximum depends upon the values of  $m$  and  $n$ .

For  $m = 0$  and  $\pm n = 0, 1, 2, 5$  and  $10$ ,  $T_{\theta\theta}(R)$  does not change much with  $n$  except at points for which  $1.13R_{in} < R \leq 1.2R_{in} = R_{ou}$ , i.e. at points near the inner surface of the everted tube; e.g. see Fig. 11. For  $n = -10, 5$  and  $10$ ,  $|T_{\theta\theta}(R_{ou})|/C_{10}$  equals  $\sim 0.7, \sim 0.8$  and  $\sim 1.1$ , respectively.

4.2.2. Affine variation of  $C_1(R)$  and  $C_2(R)$

For  $R_{ou}/R_{in} = 1.2$ ,  $\alpha = \beta = -R_{in}/(2R_{ou})$ , 0, 1, 2, 5 and 10, Fig. 12a and b evinces through-the-thickness variations of  $T_{rr}$  and  $T_{\theta\theta}$ . The magnitude of  $T_{\theta\theta}(\sqrt{R_{in}R_{ou}})$  is essentially independent of the value of  $\alpha$ . The hoop stress  $T_{\theta\theta}$  on the inner surface of the everted tube increases from  $\sim 0.3C_{10}$  to  $\sim 9.8C_{10}$  when  $\alpha$  is increased from  $-0.42$  to  $10$ . Except for  $\alpha = 10$ , the variation of  $T_{\theta\theta}$  through the cylinder thickness is affine.

For a cylinder with  $R_{ou} = 5R_{in}$ , we have plotted in Fig. 13a and b the through-the-thickness distributions of  $T_{rr}$  and  $T_{\theta\theta}$  for six different values of  $\alpha = \beta$ . With an increase in the cylinder thickness from  $0.2R_{in}$  to  $4R_{in}$ , the maximum magnitude of  $T_{rr}$  increases from

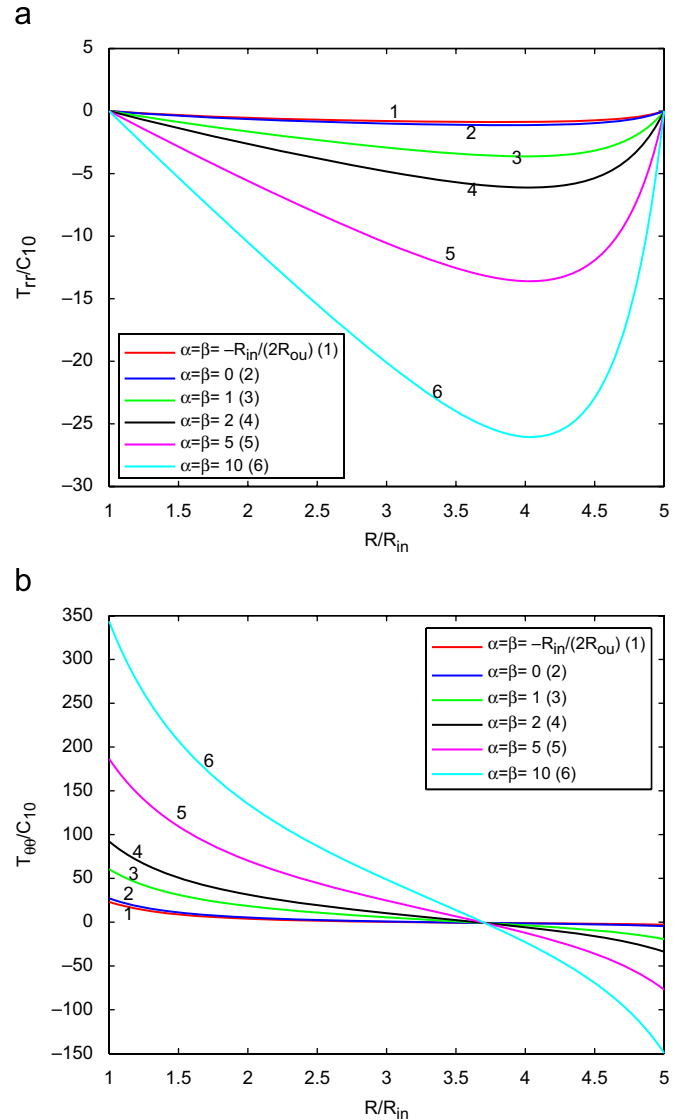


Fig. 13. For eversion of a cylinder with  $R_{ou}/R_{in} = 5$ , and  $\alpha = \beta = -R_{in}/(2R_{ou})$ , 0, 1, 2, 5, 10, through-the-thickness distributions of (a) the normalized radial stress and (b) the normalized hoop stress.

$\sim 0.43C_{10}$  to  $\sim 26C_{10}$ , and that of  $T_{\theta\theta}$  from  $\sim 10C_{10}$  to  $\sim 350C_{10}$ . These stresses are too large to be sustained by the material without failure suggesting thereby that such a large cylinder cannot be inverted without fracturing it.

For  $R_{ou} = 1.2R_{in}$  and different values of  $\alpha$  and  $\beta$  considered above, the change in the cylinder length was  $\sim 0.5\%$ , and the decrease in the cylinder thickness  $0.14\%$ . However, for  $R_{ou} = 5R_{in}$  and  $\alpha = 0$ , values of  $(D, \% \text{ change in thickness})$  were found to be  $(-0.8045, -29), (-0.8128, -28.98), (-0.8811, -28.1), (-0.9303, -26), (-1.0164, -25.2)$  and  $(-1.078, -23.92)$  for  $\beta = -0.42, 0, 1, 2, 5$  and  $10$ , respectively. The corresponding values of the inner radius of the everted cylinder equaled  $1.98, 2.013, 2.238, 2.369, 2.579$  and  $2.73$ , respectively. One can thus discern changes in the geometry of the everted cylinder.

4.3. Remarks

We have exhibited results for integer values of exponents  $m$  and  $n$  in Eq. (3.4). These results vary smoothly with changes in  $m$  and  $n$ .

If desired, one can compute the radial stress from Eq. (3.35) for non-integer values of  $m$  and  $n$ , and the hoop and the axial stresses from Eqs. (3.8)<sub>1</sub> and (3.8)<sub>2</sub>.

## 5. Conclusions

We have used a member of Ericksen's family of universal solutions to analyze radial expansion/contraction of a cylinder made of an isotropic and inhomogeneous Mooney–Rivlin material. The two material parameters are assumed to vary continuously in the radial direction either according to a power law or a polynomial of degree one in the radial coordinate  $R$  in the reference configuration. When the two material parameters are linear functions of  $R$ , the hoop stress is constant through the wall thickness. When the two material parameters increase rapidly with an increase in  $R$ , the maximum tensile hoop stress in an internally pressurized cylinder occurs on the outer surface in contrast to its occurring on the inner surface when the two parameters either decrease or slowly increase with an increase in  $R$ . For values assigned to the two material parameters, the tensile hoop stress on the inner surface of an internally pressurized thin cylinder with inner radius/thickness equal to 100 is about 300 times the applied pressure; the exact value depends upon the gradation of material parameters. For an internally pressurized cylinder with the outer radius equal to 100 times the inner radius, the tensile hoop stress on the inner surface equals eight times the applied pressure.

With a suitable tailoring of material properties in the radial direction the hoop stress can be made to be compressive on the inner surface and tensile on the outer surface, or uniform through the cylinder thickness. Thus the variation in the radial direction of the two elastic parameters in the Mooney–Rivlin constitutive relation has a dramatic effect on the stress distribution in the cylinder.

We have also studied eversion of a cylinder made of a FG material. The through-the-thickness variation of the hoop stress in the everted tube strongly depends upon the gradation of material properties. The hoop stress is not uniform through the cylinder thickness when the two elastic parameters vary linearly with  $R$ . For a thick cylinder, the thickness and the length of the everted cylinder change significantly during the eversion process.

## Acknowledgments

This work was supported by the Office of Naval Research Grant N00014-98-06-1-0567 to Virginia Polytechnic Institute and State University with Dr. Y.D.S. Rajapakse as the program manager, and by Virginia Tech's Institute for Critical Technologies and Sciences. Views expressed herein are those of authors, and neither of the funding agencies nor of their institution.

## Appendix

Expressions for the radial stress,  $T_{rr}$ , for several integer values of  $m$  and  $n$  are listed below.

Case A1:  $m = n = 5$ .

$$T_{rr} = \frac{\mu_0 A}{R_{in}^5} \left[ \frac{2}{3} R^3 - 3AR - \frac{A^2 R}{2r^2} + \frac{7}{2} A^{3/2} \tan^{-1} \left( \frac{R}{\sqrt{A}} \right) \right] + K. \quad (A1)$$

Case A2:  $m = n = 10$ .

$$T_{rr} = \frac{A\mu_0}{2R_{in}^5} \left[ \frac{R^8}{2} - AR^6 + 2A^2 R^4 - 5A^3 R^2 + \frac{A^5}{r^2} + 7A^4 \ln r^2 \right] + K. \quad (A2)$$

Case A3:  $m = n = -5$ .

$$T_{rr} = \mu_0 R_{in}^5 \left[ -\frac{1}{5R^5} + \frac{1}{A^2 R} + \frac{R}{2A^2 r^2} + \frac{3}{2A^{5/2}} \tan^{-1} \left( \frac{R}{\sqrt{A}} \right) \right] + K. \quad (A3)$$

Case A4:  $m = n = -10$ .

$$T_{rr} = -\frac{\mu_0}{2} R_{in}^{10} \left( \frac{1}{5R^{10}} - \frac{1}{3A^2 R^6} + \frac{1}{A^3 R^4} - \frac{1}{A^4 r^2} + \frac{8 \ln r}{A^5} - \frac{3}{A^4 R^2} - \frac{8 \ln R}{A^5} \right) + K. \quad (A4)$$

## References

- [1] Y. Ikeda, Y. Kasai, S. Murakami, S. Kohjiya, Preparation and mechanical properties of graded styrene-butadiene rubber vulcanizates, *J. Jpn. Inst. Metals* 62 (1998) 1013–1017.
- [2] R.C. Batra, Finite plane strain deformations of rubberlike materials, *Int. J. Numer. Methods Eng.* 15 (1980) 145–160.
- [3] J.L. Ericksen, Deformations possible in every isotropic incompressible perfectly elastic body, *Z. Angew. Math. Phys.* 5 (1954) 466–486.
- [4] R.S. Rivlin, Large elastic deformations of isotropic materials, VI: further results in the theory of torsion, shear and flexure, *Philos. Trans. R. Soc. London A* 242 (1949) 173–195.
- [5] R.C. Batra, Optimal design of functionally graded incompressible linear elastic cylinders and spheres, *AIAA J.* 46 (2008) 2050–2057.
- [6] R.C. Batra, G.L. Iaccarino, Exact solutions for radial deformations of functionally graded isotropic and incompressible second-order elastic cylinders, *Int. J. Non-Linear Mech.* 43 (2008) 383–398.
- [7] E. Bilgili, A parametric study of the circumferential shearing of rubber tubes: beyond isothermality and material inhomogeneity, *Kautsch. Gummi Kunstst.* 12 (2003) 671–676.
- [8] O. Lopez-Pamies, P. Ponte Castaneda, On the overall behavior, microstructure evolution, and macroscopic stability in reinforced rubbers at large deformations: I—theory, *J. Mech. Phys. Solids* 54 (2006) 807–830.
- [9] S.L. Passman, R.C. Batra, A thermomechanical theory for a porous anisotropic elastic solid with inclusions, *Arch. Ration. Mech. Anal.* 87 (1984) 11–33.
- [10] B.M. Love, R.C. Batra, Determination of effective thermomechanical parameters of a mixture of two thermoviscoplastic constituents, *Int. J. Plasticity* 22 (2006) 1026–1061.
- [11] C.O. Horgan, A.M. Chan, The pressurized hollow cylinder or disk problem for functionally graded isotropic linear elastic materials, *J. Elasticity* 55 (1999) 43–59.
- [12] S.G. Lekhnitskii, *Theory of Elasticity of an Anisotropic Body*, Mir Publishers, Moscow, 1981.
- [13] C.A. Truesdell, W. Noll, *The Nonlinear Field Theory of Mechanics*, *Handbuch der Physik*, III/3, Springer, Berlin, 1965.
- [14] R.W. Ogden, Non-linear Elasticity with Application to Material Modeling, in: *Lecture Notes in IPPTAN*, vol. 6, Warsaw, 2004.
- [15] A.E. Green, W. Zerna, *Theoretical Elasticity*, Clarendon Press, Oxford, 1954.
- [16] G. Arfken, *Mathematical Methods for Physicists*, third ed., Academic Press, Orlando, FL, 1985.
- [17] I-S. Liu, *Continuum Mechanics*, Springer, Berlin, 2002.
- [18] R.C. Batra, *Elements of Continuum Mechanics*, AIAA, Reston, 2005.
- [19] R.C. Batra, I. Müller, P. Strehlow, Treloar's biaxial tests and Kearsley's bifurcation in rubber sheets, *Math. Mech. Solids* 10 (2005) 705–713.
- [20] D.J. Hasanyan, R.C. Batra, S. Harutyunyan, Pull-in instabilities in functionally graded microthermoelastomechanical systems, *J. Thermal Stresses* 31 (2008) 1006–1021.